Journal of Magnetism and Magnetic Materials 321 (2009) 2197–2199

Contents lists available at ScienceDirect

Journal of Magnetism and Magnetic Materials

journal homepage: www.elsevier.com/locate/jmmm

Analytic theory of wall configuration and depinning mechanism in magnetic nanostructure with perpendicular magnetic anisotropy

Kab-Jin Kim, Sug-Bong Choe *

School of Physics, Seoul National University, Seoul 151-742, Republic of Korea

ARTICLE INFO

Article history:
Received 23 July 2008
Available online 3 February 2009

Keywords:
Ferromagnetic nanowire
Magnetic domain wall
Depinning
Perpendicular magnetic anisotropy

ABSTRACT

We present an analytic theory of the domain wall depinning in magnetic nanostructure with perpendicular magnetic anisotropy. The variational principle reveals that the wall is bent in the form of a circular arc which intersects the structure boundaries perpendicularly. The radius is inversely proportional to the magnetic field. With increasing the field the radius shrinks, followed by depinning from the constriction when the arc is not geometrically allowed. The depinning field is proportional to the sine of the constriction angle and the inverse of the constriction width. The validity of the theory is confirmed by comparison with the micromagnetic simulation.

Ferromagnetic nanostructures have drawn great technological attention for various prospective applications of the next generation memory and logic devices [1,2]. In these devices, the data are stored in the form of the magnetic domains and the domain walls. The domain walls in nanostructures propagate via the successive pinning and depinning processes from the structural constrictions [3–5]. Consequently, the threshold field for wall motion is largely determined by the nanoscale structural configuration. To precisely control the domain wall movement, it is thus crucial to understand the influence of the structural roughness on the domain wall dynamics. In this letter, we present a rigorous analytic solution of the domain wall profile in magnetic nanostructure with perpendicular magnetic anisotropy. The evolution of the wall profile with respect to an applied magnetic field is then discussed and finally, a rigorous analytic formula of the depinning magnetic field is presented.

The planar view of the typical nanowire structure with edge roughness is depicted in Fig. 1(a). Here, the right edge has the roughness with $x = w(y)$ and the left edge is assumed to be flat with $x = 0$. The flat structure of the left edge is considered only for the mathematical convenience and the theory can be easily extended for the case of both rough edges. When there exist two magnetic domains, one can intuitively imagine that the domain wall is placed at the narrowest channel under zero magnetic field. It is ascribed to the minimization of the domain wall energy with minimum domain wall length. We put $y = 0$ for minimum $w(y)$ and the two intersection points to the wire edges are denoted by $A(0,0)$ and $B(x_0,0)$ as shown in Fig. 1(b). Applying an external magnetic field H to the perpendicular direction along $\hat{z}$, the domain wall is pushed to a side to reduce the Zeeman energy. The intersection points thus move to different places as denoted by A' and $B'(x_1,y_1)$ in Fig. 1(c). The domain wall is also bent to a curve and we adopt an arbitrary function $y = f(x)$ as the wall profile.

The minimization condition of the magnetic energy is then considered to determine the domain wall profile $f(x)$. The energy difference between the two domain states shown in Fig. 1(b and c) is mainly ascribed to the change in the domain wall energy E_W and the Zeeman energy E_Z. The deviation of the other energies such as the dipolar interaction across the smoothly bent domain wall and the imperfect wall formation at rough edges is at least one order smaller than the change in E_W and E_Z, as confirmed by micromagnetic calculation [6].

The domain wall energy is simply proportional to the length of the domain wall and thus, the difference in the domain wall energy between the two configurations is given by

$$\Delta E_W = E_W(H) - E_W(0) = \sigma_W t\left(\int_0^{x_1}\sqrt{1+(df/dx)^2}dx - x_0\right), \qquad (1)$$

where σ_W is the domain wall energy density per unit area and t is the thickness of the nanostructure. On the other hand, the difference in the Zeeman energy is

$$\Delta E_Z = -2M_S Ht\left(\int_0^{x_1}(f(x)-y_1)dx + \int_0^{y_1} w(y)dy\right) - M_S H t l_W\left(\int_0^{x_1}\sqrt{1+(df/dx)^2}dx - x_0\right), \qquad (2)$$

where M_S is the saturation magnetization and l_W is the domain wall width. The first term corresponds to the area swept by the domain wall and the second term corresponds to the area occupied by the domain wall with the finite domain-wall width.

* Corresponding author. Tel.: +82 2 880 9254; fax: +82 2 884 3002.
E-mail address: sugbong@snu.ac.kr (S.-B. Choe).

0304-8853/$ - see front matter © 2009 Elsevier B.V. All rights reserved.
doi:10.1016/j.jmmm.2009.01.031

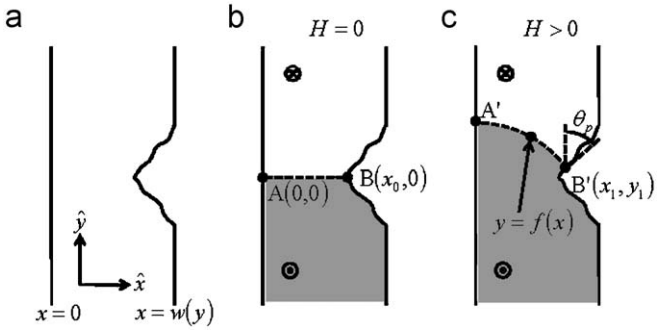

Fig. 1. (a) The planar view of the nanowire structure with edge roughness. (b) The domain structure under zero magnetic field. (c) The domain structure under an applied magnetic field *H*.

The total energy difference $\Delta E = \Delta E_W + \Delta E_Z$ is then given by

$$\Delta E = 2M_S Ht\left[\int_0^{x_1}\left(\alpha\sqrt{1+(df/dx)^2} - f(x) + y_1\right)dx - \int_0^{y_1} w(y)dy - \alpha x_0\right], \tag{3}$$

with $\alpha = \sigma_W/2M_S H - l_W/2$. The first term inside the parenthesis corresponds to the energy determined by the domain wall profile $y = f(x)$ between two end points A' and B'. The minimization condition of the first term is obtained by the calculus of variations and the corresponding Euler differential equation is

$$\frac{d}{dx}\left(\frac{\alpha(df/dx)}{\sqrt{1+(df/dx)^2}}\right) + 1 = 0 \tag{4}$$

The solution is readily obtained as $y = f(x) = \sqrt{\alpha^2 - (x - x_c)^2} + y_c$, where x_c and y_c are originally introduced as the integration constants. This equation is equivalent to $(x-x_c)^2 + (y-y_c)^2 = \alpha^2$ and thus, it proofs that the domain wall forms a circular arc of the radius α with the center (x_c, y_c).

One integration constant y_c is removed by replacing with $y_c = y_1 - \sqrt{\alpha^2 - (x_1 - x_c)^2}$, since the circular arc passes through the point B'. The other integration constant x_c is determined by the energy minimization condition i.e. $\partial(\Delta E)/\partial x_c = 0$. It can be then shown that $x_c = 0$ after some algebra. It implies that the center of the circular arc always lies on the left edge of the nanowire and consequently, the domain wall intersects the left edge perpendicularly, in accordance with the general observation in micromagnetic prediction [7]. It also explains the origin of the decalcomania domain patterns between the nanowires with the single and double notches, recently discussed elsewhere [7]. The energy difference in Eq. (3) is then consequently rewritten to

$$\Delta E = \frac{\sigma_w t}{2\alpha + l_w}\left[\alpha^2 \cot^{-1}\sqrt{\left(\frac{\alpha}{x_1}\right)^2 - 1} + x_1\sqrt{\alpha^2 - x_1^2} - 2\int_0^{y_1} w(y)dy - 2\alpha x_0\right] \tag{5}$$

after replacing the integration constants and carrying out the integration of the first term.

Fig. 2 illustrates the energy landscapes for some typical edge profiles. Here, we test a triangular notch (left) and a sinusoidal roughness (right) as plotted in Fig. 2(a). For a large α, the energy landscape exhibits the local minimum as shown by the solid lines in Fig. 2(b). The domain wall is thus pinned at the position of the local minimum. For a given α_p, the pinning position (x_p, y_p) is determined to be

$$x_p = w(y_p) = \alpha_p \sin\theta_p = \left(\frac{\sigma_W}{2M_S H_p} - \frac{1}{2} l_W\right)\sin\theta_p, \tag{6}$$

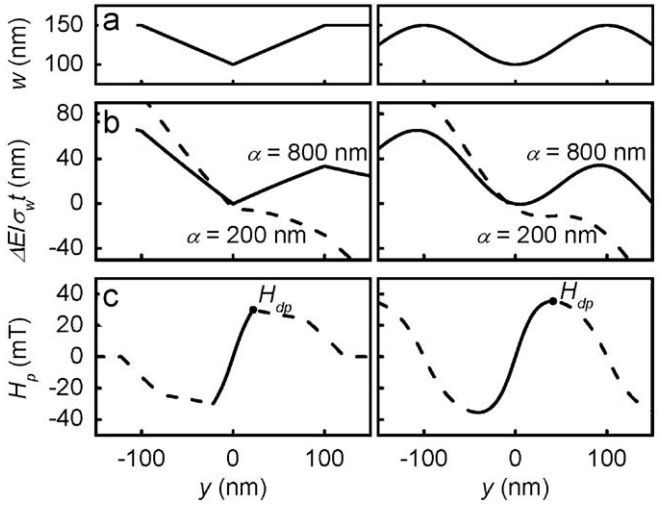

Fig. 2. (a) The edge profile $w(y)$ for a triangular notch (left) and a sinusoidal roughness (right). (b) The magnetic energy landscape ΔE for pinned case (solid line) and unpinned case (dashed line). (c) The magnetic pinning field H_p (solid line). The dashed lines show the energy maximum condition provided by Eq. (6).

Table 1
Values of the parameters for micromagnetic simulation.

Simulation parameter	Value
Perpendicular magnetic anisotropy K_U	1.0×10^5 J/m^3
Saturation magnetization M_S	2.3×10^5 A/m
Exchange stiffness A_X	1.3×10^{-11} J/m
Domain wall energy density $\sigma_W = 4\sqrt{A_X(K_U - 1/2\mu_0 M_S^2)}$	3.7×10^{-3} J/m^2
Domain wall width $l_W = \pi\sqrt{A_X/\left(K_U - 1/2\mu_0 M_S^2\right)}$	43.8 nm
Film thickness	5 nm
Cell size	2.5 nm

from the condition $d(\Delta E)/dx_1|_{x_p} = 0$, where the θ_p is the angle of the tangential line at the position, i.e. $\theta_p = \cot^{-1}(dy_1/dx_1)|_{x_p}$ as depicted in Fig. 1(c). For the case of the finite domain-wall width, θ_p is replaced by the average angle $\langle\theta_p\rangle$ over the domain wall width. Eq. (6) corresponds to the geometrical situation that the center of the circular arc is placed at the intersection point between the left edge and the tangential line. It implies that the domain walls at equilibrium always intersect both the edges perpendicularly.

Finally, the domain wall evolution with respect to an external field and the depinning mechanism from the local structural constriction are considered. Fig. 2(c) shows the local pinning field H_p with respect to the pinning position y_p obtained from Eq. (6) with the average angle over the finite domain wall width. Note that Eq. (6) provides both the energy minimum (solid line) and energy maximum (dashed line). It is seen from the figure that the pinning field exists only over a finite range. It is because the energy minimum disappears outside the range, where the circular arc with perpendicular intersection to both the edges is geometrically forbidden. Typical energy landscapes for this case are depicted by the dashed lines in Fig. 2(b). The depinning field is thus given by the maximum value of the local pinning field as

$$H_{dp} = \frac{\sigma_W}{2M_S}\,\mathrm{MAX}\left[\frac{\sin\langle\theta_p\rangle}{x_p + 1/2l_W\,\sin\langle\theta_p\rangle}\right], \tag{7}$$

where MAX[] returns the maximum value inside the parenthesis. For the case of a triangular notch, the depinning field is written

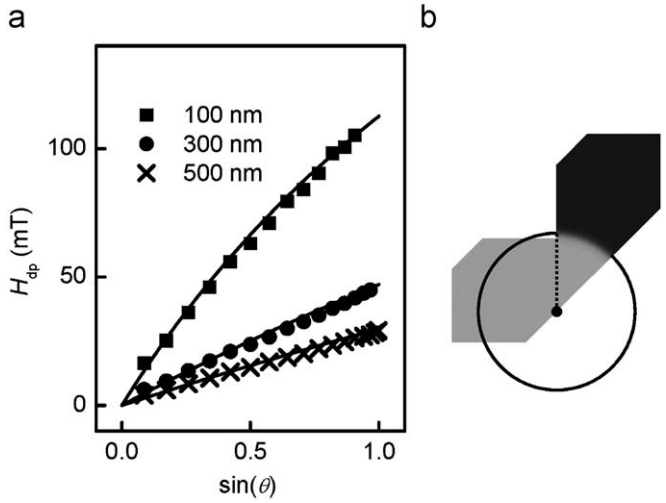

Fig. 3. (a) The depinning field H_{dp} with respect to the notch slope angle θ for several wire width as denoted in the figure. The notch depth is set to a half of the wire width. The symbols show the micromagnetic simulation results and the lines show the analytic predictions by Eq. (8). (b) Snapshot of the simulated domain configuration just before depinning. The center of the bent domain wall and the residual circular arc are drawn as guides to the eyes.

to be

$$H_{dp} = \frac{\sigma_W}{2M_S} \frac{\sin\theta}{h + 1/2l_W \sin\theta}, \tag{8}$$

where h is the minimum gap distance. The present result is consistent with the previous theory [4] for the special case of $\theta = \pi/2$ and $l_W = 0$.

To confirm the validity of the theory, micromagnetic simulation is carried out for triangular notches with varying the notch angle for several different wire widths. The simulation is performed using OOMMF [8]. The detailed simulation scheme is described elsewhere [7,9,10]. Values of the magnetic properties used in the simulation are as listed in Table 1. Fig. 3 summarizes the results. The symbols are the simulation results and the lines are the analytic predictions from Eq. (8). The quantitative coincidence between two results verifies the validity of the theory. We also confirm that the previously reported micromagnetic simulation results [7] are also quantitatively fitted to the present theory.

Acknowledgements

This study was supported by the Korea Science and Engineering Foundation through the NRL program (R0A-2007-000-20032-0). KJK was supported by the Seoul R&BD program.

References

[1] S.S.P. Parkin, M. Hayashi, L. Thomas, Science 320 (2008) 190.
[2] D.A. Allwood, G. Xiong, C.C. Faulkner, D. Atkinson, D. Petit, R.P. Cowburn, Science 309 (2005) 1688.
[3] F. Cayssol, D. Ravelosona, C. Chappert, J. Ferré, J.P. Jamet, Phys. Rev. Lett. 92 (2004) 107202.
[4] J. Wunderlich, D. Ravelosona, C. Chappert, F. Cayssol, V. Mathet, J. Ferré, J.-P. Jamet, A. Thiaville, IEEE. Trans. Magn. 37 (2001) 2104.
[5] S.-B. Choe, D.-H. Kim, K.-S. Ryu, H.-S. Lee, S.-C. Shin, J. Appl. Phys. 99 (2006) 103902.
[6] The magnetostatic energy contains a part of the wall energy, as given by $-\mu_0 M_S^2 l_W/\pi$ per unit area. Excluding this contribution, the remained deviation in the magnetostatic energy is confirmed to be about 30 times smaller than the sum of the wall energy and the Zeeman energy.
[7] S.-B. Choe, Phys. Status Solidi (c) 4 (2007) 4433.
[8] M. Donahue, D. Porter, version 1.2a4, see ⟨http://math.nist.gov/oommf/⟩.
[9] S.-B. Choe, J. Magn. Magn. Mater. 320 (2008) 1112.
[10] To clearly define the notch angle, we rotate the sample rather than rotate the notch to avoid the effect from the discrete simulation cells. The notch is thus fixed to a position in the simulation grid with clear and identical edge profile.